



Investigating the strength effects of drilling in tempered glass

A first step towards a novel dowel joint

Jens H. Nielsen · Martin J. Meyland · Bjørn E. Thorup ·
Alexandru Zugravu · John F. Olesen

Received: 6 June 2018 / Accepted: 8 January 2019 / Published online: 22 January 2019
© Springer Nature Switzerland AG 2019

Abstract The tempering process introduces a residual stress field to the glass that only allows a drilling depth of approximately 20% of the thickness (compressive zone) before fragmentation will be initiated. The present paper investigates post-drilled holes in tempered glass that can be used for a novel assembling technique leading to an increased accuracy in the connection and avoiding custom made solutions with holes drilled prior to tempering. The partly drilling is first studied experimentally measuring the change in strains (stresses) on the surface close to the hole as function of drilling depth. These data are then further used to validate a finite element model capable of describing the redistribution of residual stresses around the hole for several geometric variations such as depth, diameter, rounding and inclination. Above all, the numerical study shows an increase in the apparent strength (The

term “apparent strength” is used for the strength originating from both the material strength and the residual stress state) of the hole. Furthermore, it is seen that drilling into the compressive zone only, will not lead to any tensile stresses at the surface of the hole. As the drilling process will damage the glass around and inside the hole, hence decreasing the strength, an etching technique is finally given to post-improve the quality of the hole surface locally. After 6 h of local etching with ammonium hydrogen fluoride (NH_4HF_2), an increase in strength of about 310 % is observed. Increasing the etching time further, with the given acid and concentration, is shown not to yield any further (significant) increase in the strength.

Keywords Tempered glass · Toughened glass · Thermally pre-stressed glass · Residual stress · Drilling · Numerical modelling · Etching · Surface enhancement · Flexural testing · Joints · Connections · Stress redistribution

J. H. Nielsen (✉) · M. J. Meyland · B. E. Thorup ·
A. Zugravu · J. F. Olesen
Department of Civil Engineering, Technical University of
Denmark, Brovej, Building 118, 2800 Kgs. Lyngby,
Denmark
e-mail: jhn@byg.dtu.dk

Martin J. Meyland
e-mail: majeme@byg.dtu.dk

Bjørn E. Thorup
e-mail: bthorup@gmail.com

Alexandru Zugravu
e-mail: alexzugs@gmail.com

John F. Olesen
e-mail: jfo@byg.dtu.dk

1 Introduction

One of the main challenges when using glass is the assembling with other pieces of glass or other materials. In tempered glass, all holes need to be drilled prior to the tempering process otherwise the glass would fragmentize due to the release of stored strain energy in the glass, see e.g. Nielsen et al. (2009), Nielsen (2017), Nielsen and Bjarrum (2017) and Pourmoghaddam and

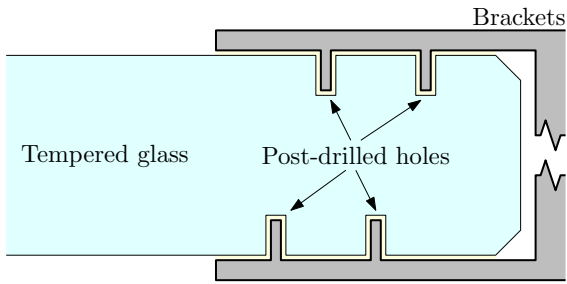


Fig. 1 Principal sketch of a possible way to attach a bracket to tempered glass with post-drilled holes

Schneider (2018). Not only does this require many tempered glass products to be custom made due to assembling, but also the high temperatures involved in the tempering process may lead to geometrical inaccuracies of hole placements etc. which eventually needs to be accounted for using oversize holes in combination with a filler material.

This paper investigates how the local residual stress state in tempered glass is affected by drilling. By only drilling partly through the glass, holes are stable and may be used for assembling and transferring loads. Especially since the apparent strength (The term “apparent strength” is used for the strength originating from both the material strength and the residual stress state) of the glass in the vicinity of the hole can be higher than first expected due to a favourable redistribution of residual stresses. A possible way of designing

a bracket connection in tempered glass utilising such holes is illustrated in Fig. 1.

The present paper considers the drilling of a hole in tempered glass, how it affects the strength and how the strength can be improved by acid etching.

1.1 Redistribution of residual stresses

The local redistribution of stresses due to the drilling may be estimated analytically. If a large pane, relative to the diameter of the hole, in pure in-plane compression is considered, an analytical solution to this problem can be derived for the radial and tangential stresses respectively as function of the radius, r , see e.g. Timoshenko and Goodier (1970)

$$\sigma_r(r) = \left[1 - \left(\frac{a}{r}\right)^2 \right] \sigma_\infty \tag{1a}$$

$$\sigma_\theta(r) = \left[1 + \left(\frac{a}{r}\right)^2 \right] \sigma_\infty \tag{1b}$$

where a is the hole radius and σ_∞ is the far-field residual stress. An illustration of the geometry for a partly drilled hole and the appertaining far-field stress is given in Fig. 2.

In such pane the stress state at any given point will be equibiaxial, i.e. in a cylindrical coordinate system: $\sigma_\theta = \sigma_r = \sigma$ and $\sigma_z = \tau_{r\theta} = 0$.

Obviously the assumptions of a homogeneous stress state and a hole through the thickness is not valid in

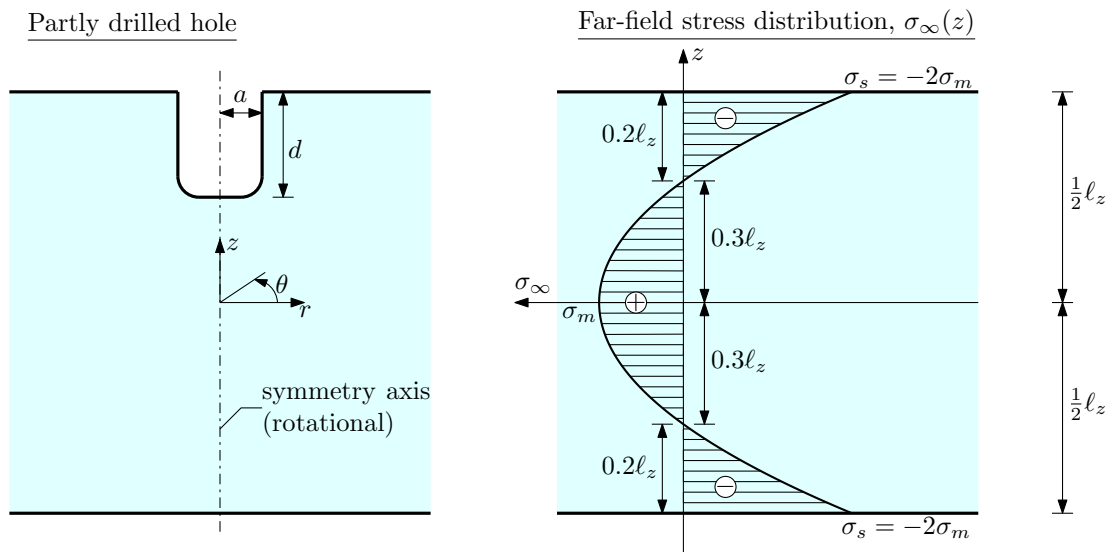


Fig. 2 Geometry of a partly drilled hole (left) and a sketch of the far-field residual stress distribution (right)

this investigation, however, for a small hole diameter, $2a$, and a relatively deep hole the influence from the assumptions vanishes on the boundary of the hole near the surface.

From Eq. (1a) it is seen that the radial stress, σ_r , on the boundary of the hole ($r = a$) is zero as expected on a free surface. However, the tangential stress, σ_θ , at the hole boundary is doubled. Since the apparent strength of tempered glass is governed by the residual stresses, this leads to a considerable local increase in apparent strength. Consider the important case of equibiaxial bending where the stress concentration around such a hole is a factor of two, the strength originating from the residual stress will therefore not be reduced. The hole will introduce considerable damage/flaws to the glass surface and the inherent glass strength will therefore be low. However, this can be improved by acid etching locally at the hole as experimentally shown later.

This investigation is limited in the way that the effect is only studied far from edges (more than two times the thickness) and the residual stress state can be approximated fairly accurate by a symmetric parabola fulfilling the equilibrium condition $\int_0^t \sigma_\infty(z) dz = 0$, namely:

$$\sigma(z) = \left(1 - \frac{12}{\ell_z^2} z^2\right) \sigma_m = \left(\frac{6}{\ell_z^2} z^2 - \frac{1}{2}\right) \sigma_s \quad (2)$$

where σ_m and σ_s represents the mid plane stress and the surface stress respectively. From this approximation some typical properties for the farfield residual stress state can be derived:

- The compressive surface stress is twice the mid-plane tensile stress in magnitude $\sigma_s = -2\sigma_m$
- The centre tensile zone is about 60% of the thickness ($\frac{\ell_z}{\sqrt{3}} \approx 0.6\ell_z$), which indicates that the depth from the surface where the residual stress becomes zero is approximately 20% through the thickness.

The far-field stress is assumed homogeneously distributed far from edges/holes. This is not always the case for commercially tempered glass where large variations can be found as reported by e.g Nielsen et al. (2010b) and Veer and Rodichev (2014). However, the holes considered in this paper are small and only influence the stress state locally and the assumption of a homogeneous residual stress field seems reasonable.

2 Experimental—drilling

In order to experimentally test the idea and theory stated, the residual stress state needs to be measured at least before and after drilling. Measuring the residual stresses prior to drilling can be done relatively easy by a scattered light polariscope (Anton and Aben 2003) since glass is a so-called photo-elastic material (Aben and Guillemet 1993). However, this device is difficult to use for measuring the residual stresses during and after the drilling. Instead the change in strain (stress) during the drilling was measured by a small strain gauge installed near the hole. These experiments were then used for validating a Finite Element (FE) model of the problem which could then be further explored in a parametric study.

2.1 Experimental setup

Four specimens were considered for validating the FE model. Each specimen was 350 mm × 350 mm × 10 mm and prior to drilling, the residual stresses were measured using a scattered light polariscope (SCALP-04) in two orthogonal directions at the centre point for the drilling. The strain gauge was applied for measuring the change in surface strain (tangential direction), $\varepsilon_\theta^{\text{top}}$, at a location as specified in Fig. 3 and Table 1. The placement of the strain gauge is important when validating the FE-model which will be discussed later.

After measuring the residual stresses, a strain gauge was installed on the glass close to where the drilling of the hole was planned. For the first two specimens a standard size strain gauge (Micro-Measurements EA-06-060LZ-120/E) was used. However, due to high strain gradients in the area, a smaller strain gauge (Tokyo Sokki Kenkyujo FLK-1-11) was used for the last two specimens. The distance to the drilled hole was measured after drilling for increasing accuracy. All results related to the drilling are reported in Table 1 where $\Delta\sigma_\theta^{\text{top}}$ and σ_s^{top} denotes the change in surface stress after drilling and the residual surface stress measured before drilling. A $\phi 1.8$ mm diamond coated solid tip drill was used. The exact diameter of the hole is likely to be slightly larger than the diameter of the drill due to inaccuracy of the machine. However, this was not measured. Accurate measurements of the distance between hole and strain-gauge was also difficult to achieve as the hole perimeter was not well defined due to local chipping of the glass.

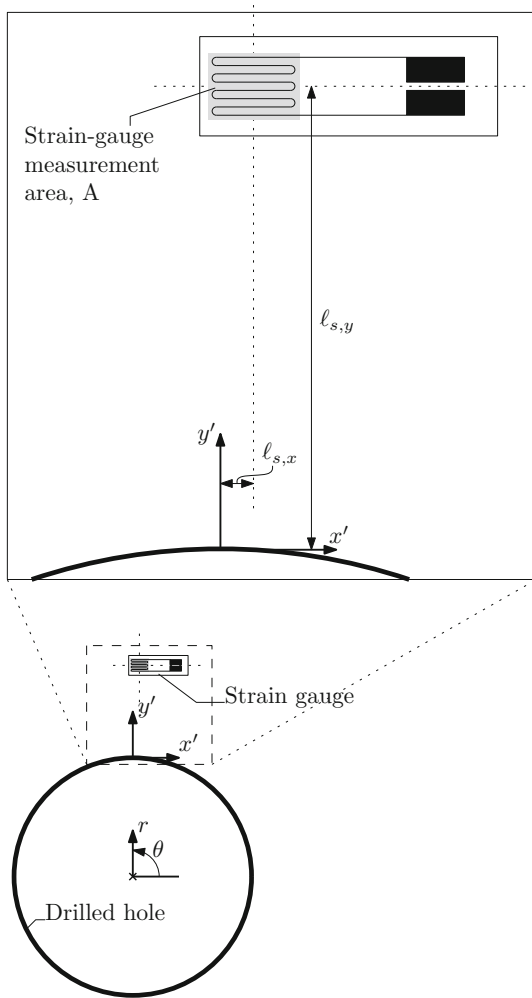


Fig. 3 Location of measurement points and strain gauge

Since water was needed during drilling, the strain gauge was coated using a silicone rubber (HBM SG250) which needed to cure before reliable data could be obtained. In order to determine the effect of curing, data from the strain gauge was logged dur-

Table 1 Experimental data from the four drilling tests. The strain gauge type and dimensions are given along with experimental data for the drilling depth (d), strain gauge location ($\ell_{s,y}$), change

ing the curing of the silicone and by means of those results an acceptable steady response was found after approximately 20 h, see Fig. 4a. After curing of the silicone rubber, a ring of plasticine was formed around the drilling area and filled with water for cooling/cleaning during the drilling process. The influence from the water (different temperature) was stabilised after 40 s, which is shown in Fig. 4b.

Drilling was done step-wise in order to allow the water to remove the drill dust. The step-wise drilling is seen in Fig. 5 showing the strain gauge response (converted to stress) as function of time for one of the experiments (specimen 3); note that the red curve is related to the right vertical axis providing the drilling depth, d . Looking at the stress curve, small local spikes are seen which can be explained by the step-wise drilling procedure where pressure is put on the drill at these exact times (compare with the drilling depth curve).

In order to extract data for a relation between the measured change in stress at the surface, $\Delta\sigma_\theta^{\text{top}}$, and the drilling depth, the points in Fig. 5 marked by a circle (for the drilling depth) and a cross (for the change in stress) are paired in Table 2. The location of these points are selected manually after the effect from the pressure of the drill has been removed.

3 Numerical modelling—drilling

In previous work (Nielsen 2012, 2013) a numerical model for the drilling in tempered glass was established and used, but not validated. In the references, a state-of-the-art model for establishing the residual stress state was used (Nielsen et al. 2010a). However, in this paper the determination of the residual stress state is not the focus and therefore a simpler approach is applied where the stress state is specified directly by a temperature field and a suitable thermal expansion.

in surface stress due to drilling, ($\Delta\sigma_\theta^{\text{top}}$) and measured surface stress before drilling (σ_s^{top})

Specimen	Strain gauge	Gauge dim. (mm × mm)	d (mm)	$\ell_{s,y}$ (mm)	$\Delta\sigma_\theta^{\text{top}}$ (MPa)	σ_s^{top} (MPa)
1	EA-06	1.52 × 1.90	2.18	1.39	− 6.44	− 70 (± 1.72)
2	EA-06	1.52 × 1.90	2.05	2.03	− 5.07	− 70 (± 0.37)
3	FLK-1-11	1.00 × 0.70	2.15	0.7	− 17.97	− 72 (± 0.34)
4	FLK-1-11	1.00 × 0.70	2.09	0.7	− 16.80	− 70 (± 2.54)

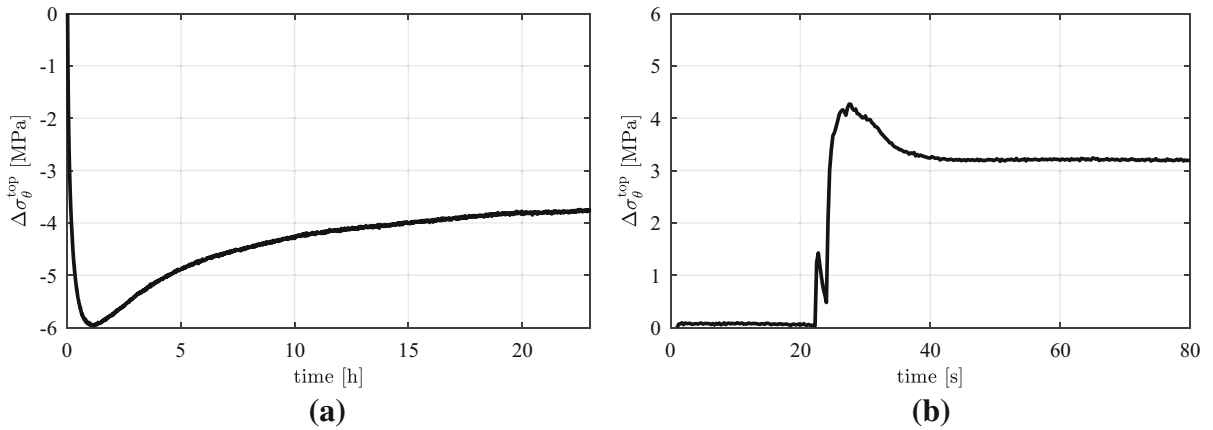


Fig. 4 Effect on stress measured through strain gauges as a function of time. Left (a) silicone coating and Right (b) water applied for drilling. It should be noted that the initial stresses in the plots

are subtracted, leaving only the effect from the considered phenomenon to be shown

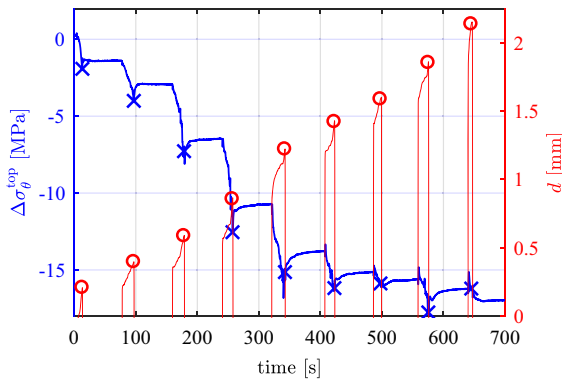


Fig. 5 Change in tangential stress (left axis) and drilling depth (right axis) as function of time for specimen 3. It should be noted that the initial stress in the plot is set to zero, leaving only the effect from the considered phenomenon to be shown. Points marked by a circle (for the drilling depth) and a cross (for the change in stress) are paired in Table 2

For modelling the stress redistribution due to the drilling, an axi-symmetric model is developed. The residual stress distribution over the thickness is given

in Eq. (2). This residual stress distribution is a reasonable assumption far away from any edges and in thin panes where the transverse stress component can be assumed zero. In an axi-symmetric model where only stresses far from the edges are considered, this stress profile can be given as initial stresses, typically by an artificial initial temperature state. The relation between temperature and stress follows as

$$\sigma(z) = \frac{E}{1 - \nu} \alpha \Delta T(z) \tag{3}$$

where α is the coefficient of thermal expansion, E is Young’s modulus, ν is Poisson’s ratio and $\Delta T(z)$ is a temperature change distribution with the same shape as the residual stresses from Eq. (2). The following properties are applied to the FE model for the soda-lime-silica glass: $E = 70$ GPa and $\nu = 0.23$. The term $\alpha \Delta T(z)$ from Eq. (3) is only used for generating the residual stress state and the choice of these two parameters do not represent the physical properties. The parameters were chosen to obtain a parabolic stress state where the surface compression is -100 MPa and

Table 2 Drilling depth and measured change in residual stress at the surface by strain gauge for test 3 and 4. The units are mm and MPa respectively

Set	1	2	3	4	5	6	7	8	9	10
3: d	0.21	0.40	0.59	0.86	1.22	1.42	1.59	1.85	2.14	
3: $\Delta\sigma$	-1.92	-4.00	-7.28	-12.54	-15.14	-16.18	-15.88	-17.76	-16.21	
4: d	0.19	0.36	0.59	0.80	0.97	1.20	1.39	1.58	1.79	2.08
4: $\Delta\sigma$	-2.46	-5.13	-8.78	-11.96	-12.79	-15.71	-15.27	-15.78	-15.90	-16.16

the mid plane tensile stress is 50 MPa for the parametric studies in the present paper. Considering the validation model in the next section, stress values were measured in the specimens prior to drilling (≈ -71 MPa) and this value was used to define the initial stress state in the FE model.

In the initial step of the FE calculation, the model should only represent the state far away from the edges and a special boundary condition is needed for modelling this. This boundary condition should simply allow for all nodes on the boundary furthest away from the rotational axis, see Fig. 9, to only move uniformly and horizontally. More specifically, the following condition should be fulfilled on the boundary

$$\frac{\partial u_r}{\partial z} = 0 \tag{4}$$

In general $u_r \neq 0$, but uniformly distributed. This condition is obviously not necessary if the plate model is sufficiently large. However, this condition can be used for reducing the degrees of freedom in the model, speeding up the calculation time considerably.

3.1 Validation

Comparing the measurements from the strain gauge with numerical results for a hole with a diameter of 1.8 mm, is done in this section to validate the applied model. As discussed in Sect. 2, the exact location of the strain gauge along with the actual hole diameter was difficult to determine due to flaws generated by the drill. If the distance to the strain gauge from the boundary of the hole is measured, the influence on stresses from the hole diameter is small and can be neglected for small variations. However, the stresses vary with the location of the strain gauge.

From the axi-symmetric model this variation can be investigated. Variation of $l_{s,y}$ is straight forward and only requires that the strain is averaged over the area of the strain gauge, A . When considering the variation of $l_{s,x}$, a new distance, l_s , to the hole needs to be calculated and the stresses rotated accordingly before averaging over the strain gauge area. This is illustrated in Fig. 6.

The graphs showing the stress variations are given in Figs. 7 and 8 where the tangential residual stress, $\sigma_\theta^{\text{top}}$, is plotted as function of the drilling depth, d , for strain gauge locations varying $l_{s,x}$ and $l_{s,y}$ (see Fig. 3).

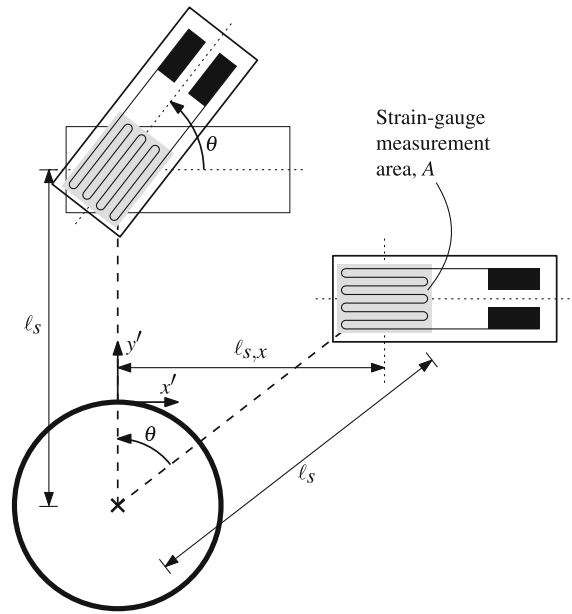


Fig. 6 Illustration of how the strains are determined from the axi-symmetric model for the variation of $l_{s,x}$

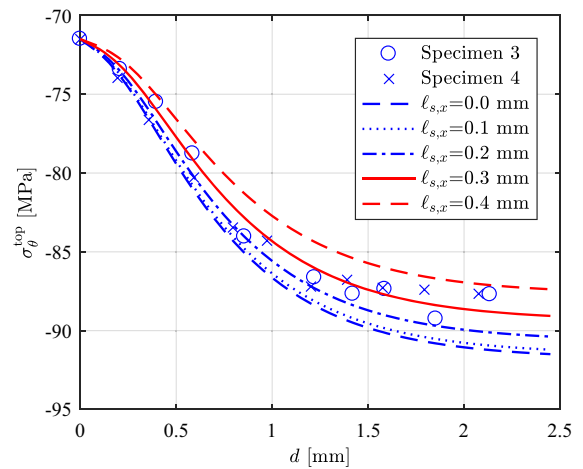


Fig. 7 FE results compared to experiments. The different curves are models where the parameter $l_{s,x}$ from Fig. 3 is varied and $l_{s,y}$ is kept constant at 0.7 mm

From these figures it is seen that a variation of the location perpendicular to the boundary of the hole results in larger tangential stress changes compared to a similar variation parallel to the hole. This seems reasonable as the stresses along $l_{s,y}$ somewhat will approach the far-field residual stress, whereas the stresses along $l_{s,x}$ experiences minor changes, since they remain close to the hole within the variation studied.

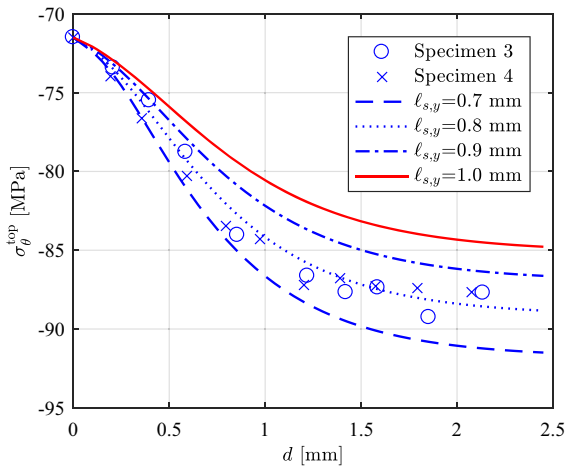


Fig. 8 FE results compared to experiments. The different curves are models where the parameter $l_{s,y}$ from Fig. 3 is varied and $l_{s,x}$ is kept constant at 0.0 mm

The applied numerical model is validated against the experimental results, see Figs. 7 and 8. Both experiments show a small scatter of the results that can be explained by the recording of the two signals (change in stress and depth) where a small time delay was present. Also, the recording frequency has caused that not all data points around the peaks have been recorded. However, the experimental results are still comparable with the numerical ones. A variation of the location along $l_{s,x}$ reveals that the strain gauges used in the experiments might have been placed with a small misalignment of about 0.3 mm. An exact measurement of this location does not exist. However, the measured strains follow the numerical results quite well indicating that the model is able to produce reliable results. Same behaviour is seen for the strains where the location along $l_{s,y}$ is varied. From the experiments the location of the used strain gauges is measured to $l_{s,y} = 0.7$ mm (see Table 1) which is not in line with the numerical results stated, when comparing the strains. According to them, the experimental results coincide with the strains calculated at a distance of about 0.8 mm. However, the numerical and the experimental results are in good agreement, thus the model is considered applicable for a parametric study.

4 Parametric investigation

The validated FE-model will in the following be applied for investigating different hole geometries in a glass

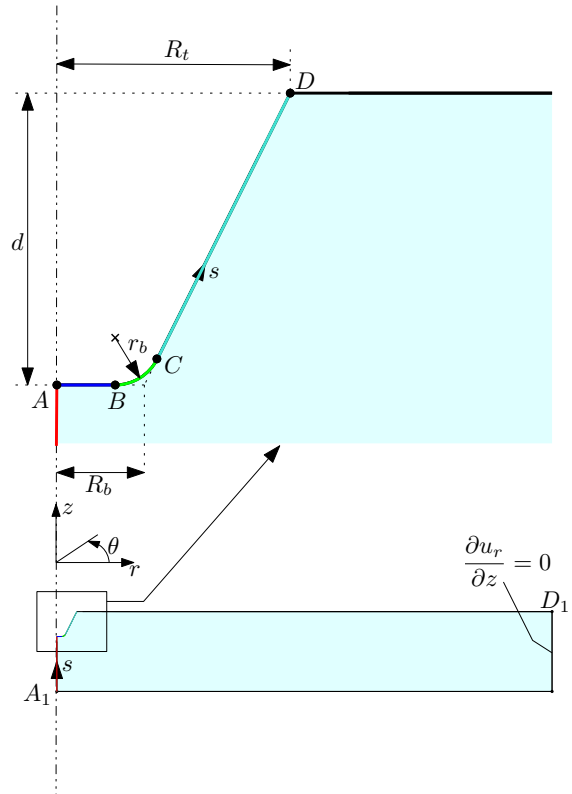


Fig. 9 Parameters for the hole geometry. Note that s is a coordinate following the boundary of the hole starting in A_1 and ending in D_1 passing through the points: A, B, C and D . Colors are used for identifying parts of plots in later figures

plate with a thickness of 10 mm. A general sketch of a partly drilled hole can be found in Fig. 9 which shows the geometry and the coordinate s along the boundary of the hole. Certain points of interest are given along the coordinate s (A_1, A, B, \dots) to be used for presenting the results.

The model is based on what is described previously in Sect. 3. The used elements are axi-symmetric second order displacement triangles (CAX6 in Abaqus) and the typical element side length in the region of the hole is approximately 0.01 mm. A typical mesh in the region of the hole can be seen from Fig. 10.

It seems obvious to compare the analytical model given in Eqs. (1a) and (1b) with the numerical model just described. However, due to differences in assumptions—such as the stress state and the depth of the hole—for the two models, the analytical model is only valid for this problem at the very perimeter of the hole along the surface of the glass. Large deviations exist just a short distance from the hole as shown

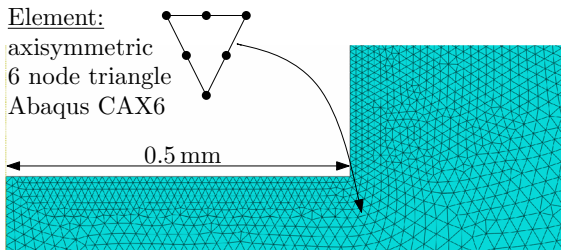


Fig. 10 Typical mesh in the region near the hole. The element side-length along the boundary of the hole is approximately 0.01 mm

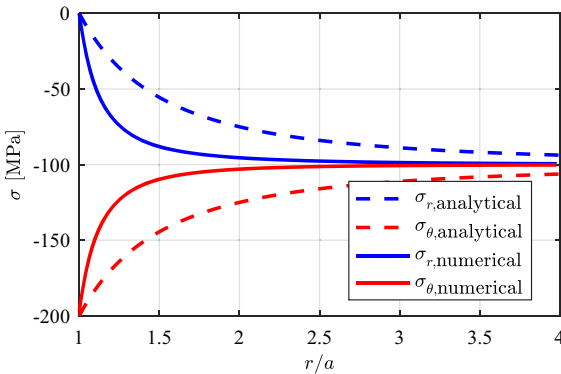


Fig. 11 Analytical and numerical comparison of surface stresses evolving from the boundary of a hole. Only at the point $\frac{r}{a} = 1$ and for $\frac{r}{a} \rightarrow \infty$ the results match

in Fig. 11, where the analytical expressions are plotted together with numerical results. A match in results is only seen at the boundary of the hole and far away from it.

4.1 Cylindrical hole with sharp corners

An important parameter to investigate, is the stress state as we vary the drilling depth, d , and the radius of the hole, $R = R_t = R_b$. The bottom corner is sharp indicating that $r_b = 0$ why the points B and C will coincide and in this section be referred to as point BC .

From Fig. 12 it is seen, as expected from St. Venant’s principle, that the radial stress is undisturbed on the bottom side ($s = 0$) of the glass even for a hole depth of 3 mm corresponding to 30% of the thickness. A negative stress singularity in the bottom corner, point BC , is seen as expected. In a drilled hole, the corner will practically always be rounded and therefore the stresses will be finite as demonstrated in Sect. 4.2. It is also worth noting that the stresses are almost back to the initial

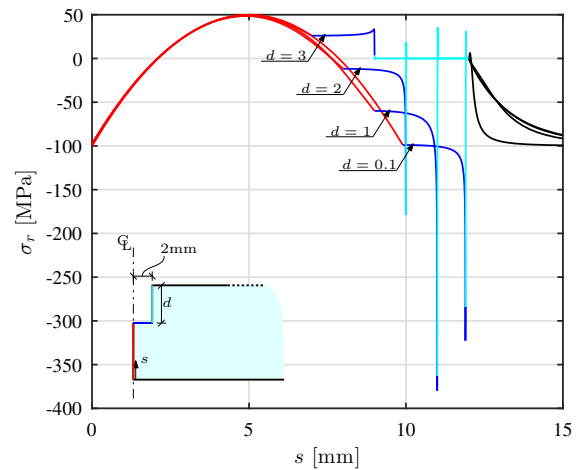


Fig. 12 Radial stresses, σ_r , as function of the coordinate s for a cylindrical hole

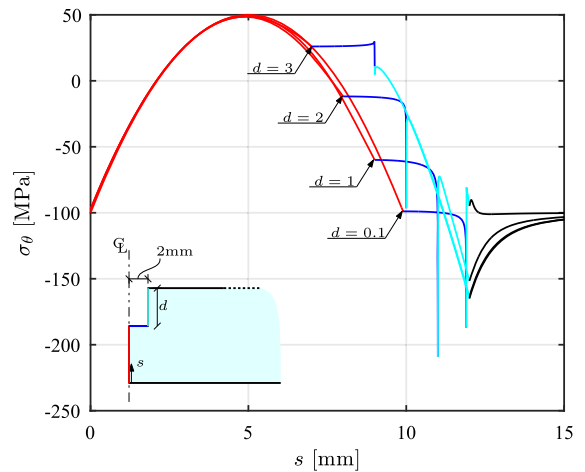


Fig. 13 Tangential stresses, σ_θ , as function of the coordinate s for a cylindrical hole

state at approximately 3 mm from the edge of the hole ($s = 15$ mm). The numerical results also indicate that a hole with a depth of 3 mm will result in positive residual stresses in the bottom of the hole (point A to BC), where an energy release and failure of the glass would be expected. However, including this depth to the study seems plausible as an experimental investigation on the maximum bore hole depth with three specimens in total showed that for a cylindrical hole it was possible to reach a depth of 29.6% ($\pm 0.2\%$) of the plate thickness before failure occurred.

Considering the tangential stress, σ_θ , in Fig. 13, the sharp inward corner at the bottom of the hole is seen to give rise to a compressive stress singularity. It is

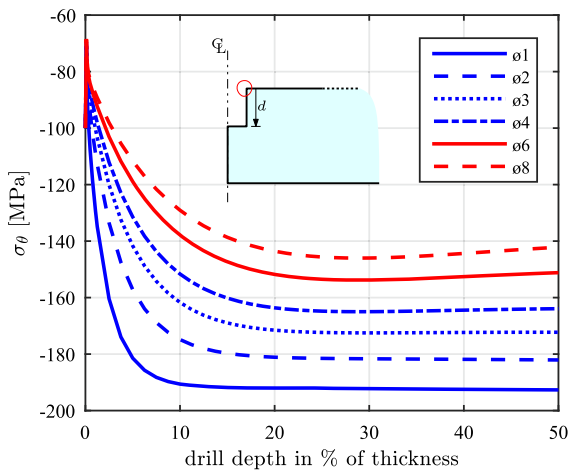


Fig. 14 Tangential stresses at the hole corner (point D , marked with a red circle) as function of drilling depth for different hole diameters (in mm)

also seen that the magnitude of the compressive tangential stress, σ_θ , in point D varies from -100 MPa to -160 MPa indicating a higher apparent strength locally. Even though this local increase in residual compressive stress is beneficial for the apparent strength in the tangential direction, the local residual radial stress will be zero due to the free surface which is also seen from Fig. 12.

A typical loading situation such as bending of the plate or shear load on a pin in the hole would primarily lead to local stresses in the tangential direction, especially in point D . The increase in compressive pre-stress at this point might be utilised leading to an increase of apparent strength. However, the effect of the drilled hole leads to stress concentrations which are of major concern for brittle materials like glass.

The above mentioned results are only for a hole radius of 2 mm ($\phi 4$) and it is interesting what will happen for other hole diameters and how stresses locally evolve during the drilling.

Figure 14 shows the tangential stress in point D as function of the drilling depth for various hole diameters. It is seen from the figure that the compressive stresses decrease in the beginning of the drilling process. However, these results in the beginning might not be precise since the drilling depth is comparable to the element size. It is interesting, but also expected from the theory, to see that for a small hole diameter and a deep hole we approach the theoretical value of twice the initial surface compressive stress which is -100 MPa. From the graph it is seen that drilling 20% of the thickness into

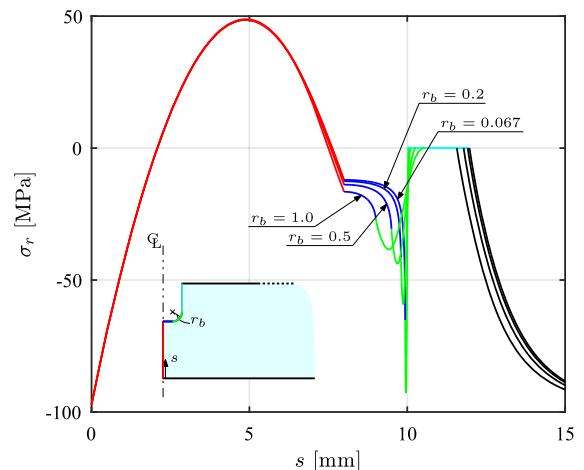


Fig. 15 Radial stresses, σ_r , as function of the coordinate s for a cylindrical hole with rounded corners at the bottom

the glass provides a reasonable increase in compressive residual stress in the vicinity of the hole and this drilling depth has been reached in experiments without any problems of fragmentation. Also, drilling deeper than that leads to no remarkable changes in residual compressive stresses as they remain almost constant for all diameters shown. A maximum drilling depth is though reached at about 20% of the thickness.

4.2 Cylindrical hole with rounded corners at the bottom

The cylindrically shaped hole is not the only possible geometry and other geometries could perform better. In order to remove the singular point at the bottom corners of the hole, this part was rounded and the effect was investigated for a fixed drilling depth of $d = 2$ mm and hole radius of $R = R_t = R_b = 2$ mm. The results are given in Figs. 15 and 16 for the radial and tangential stresses, respectively.

As shown, even a slight rounding of the corner will change the stress singularity into a stress concentration where we actually get finite stresses. It is worth noting that these stress concentrations all lead to an increase in the compressive stresses, which is usually not a problem for glass. The variation of the corner radius has no remarkable influence on the tangential stresses. However, a small increase in apparent strength is observed when increasing the radius.

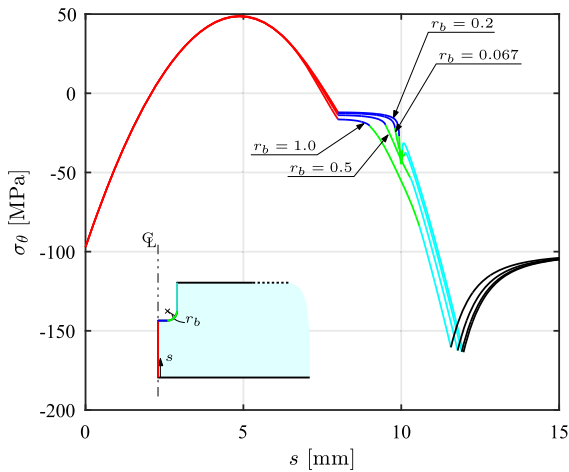


Fig. 16 Tangential stresses, σ_θ , as function of the coordinate s for a cylindrical hole with rounded corners at the bottom

If we drill deeper and into the tensile zone, the stress would locally turn into tensile stresses and the glass would fail contrary to the increase in apparent strength seen.

4.3 Cylindrical hole with inclined sides and rounded corners at the bottom

Another shape to investigate is a hole with inclined sides and rounded corners at the bottom. The inclination is defined by the value of R_b as shown in Figs. 17 and 18. For $R_b = 2.0$ the hole becomes cylindrical. The rounding of the bottom corner is kept constant at $r_b = 0.133$ mm. The radial stresses, σ_r , will obviously equal zero at the top edge of the hole (point D on Fig. 9) when $R_b > R_t = 0$ due to the free edge which is also seen on the plot. It is also worth noting that the stresses influenced by the drilling again are compressive and that they remain such (or zero). Due to the rounding of the bottom corner a stress concentration with finite stresses will arise again in that specific point. However, they are not affected by the change in inclination and remain unchanged.

Another behaviour is seen for the tangential compressive stresses as shown in Fig. 18. Increasing the parameter R_b leads to an increase in the apparent strength. At point D the strength varies from -140 to -175 MPa and subsequently the stresses approach the far-field residual stress, as expected. Again, the variation of the inclination has no significant effect on the stresses near the bottom corner.

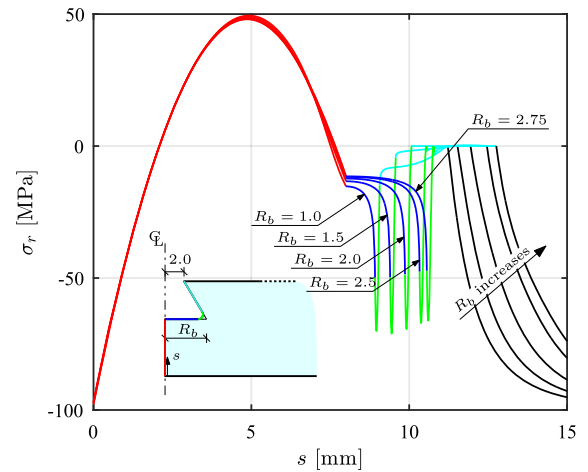


Fig. 17 Radial stresses, σ_r , as function of the coordinate s for a cylindrical hole with inclined sides and rounded corners at the bottom

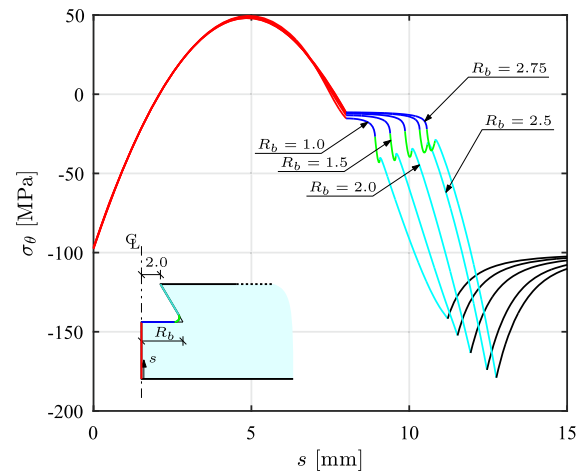


Fig. 18 Tangential stresses, σ_θ , as function of the coordinate s for a cylindrical hole with inclined sides and rounded corners at the bottom

5 Enhancement of hole surface quality

It is well-known for glass that its inherent strength is highly affected by the surface condition such as the flaw sizes and their distribution (Petzold et al. 1990). The drilling process using a diamond coated drill will introduce local flaws around and inside the hole leading to stress concentrations hence reducing the apparent strength. This section will discuss a possible way of enhancing the surface quality of the borehole. Previous studies (Proctor 1962; Saha and Cooper 1984; Kolli et al. 2009) showed that the strength of glass could

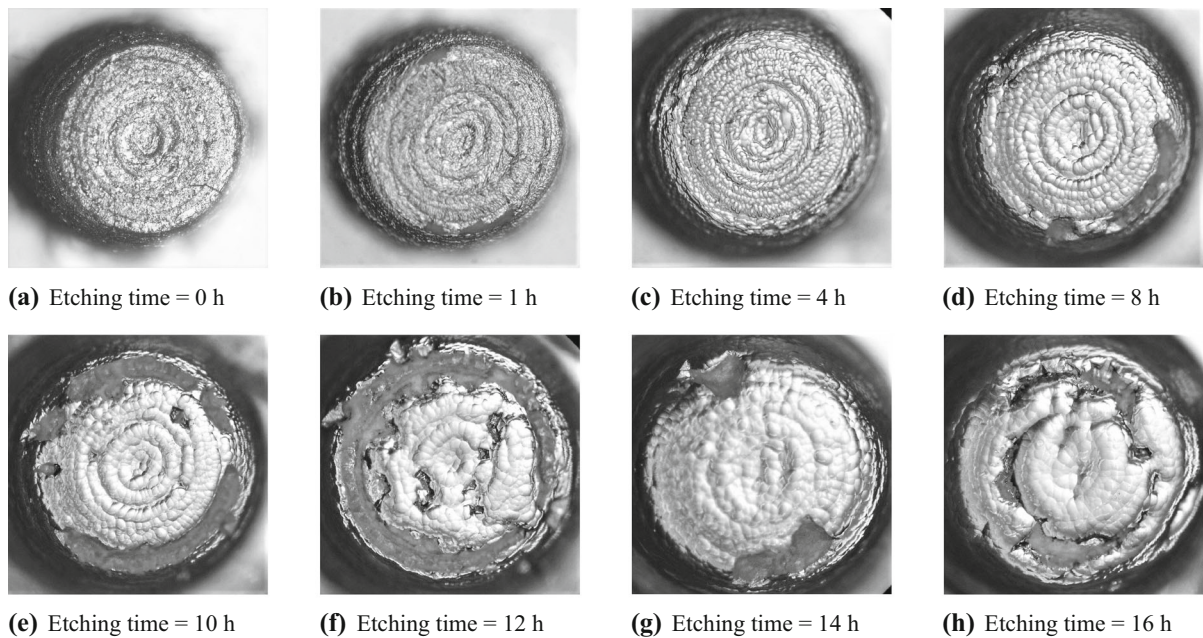


Fig. 19 Microscopic images of 8 boreholes with a diameter of 2 mm that have been exposed with different etching times

be increased by etching the surface with hydrofluoric acid (HF). A similar, but less toxic acid named ammonium hydrogen fluoride (NH_4HF_2 , 15%) was used in this investigation. The chemical reaction between the acid and silica (main component of soda–lime–silica glass) leads to the formation of silicon tetrafluoride and ammonium fluoride. The chemical reaction is



Etching the glass surface will smoothen or even completely remove the introduced flaws. This effect was used to locally strengthen the boreholes. The main objectives of this study were to develop a proper technique to locally etch the holes and to see the effect of different etching times on the flexural strength. All experiments conducted, were based on 28 specimens all having a centrally placed $\varnothing 2$ mm hole with a depth of $d = 1.8$ mm. The overall dimensions of each specimen were 400 mm \times 250 mm \times 10 mm.

5.1 Etching procedure

Previous studies related to etching of glass surfaces, immersed the whole specimen into a bath with acid, which was not an applicable procedure for this inves-

tigation. Therefore, a new technique was developed to perform a local etching.

Prior the etching, a strip of adhesive tape was placed around the hole preventing the surrounding surface to get in contact with the acid, which was filled into the cleaned hole immediately afterwards. To avoid evaporation of water, the hole was covered with a small cap to stop that. In the beginning of the etching procedure, every 15 minutes new acid was added to the hole to ensure a continuous etching. However, after 30 minutes the hole needed to be cleaned and new acid was added, as the chemical reaction formed crystals that disturbed the reaction. This was repeated after 60 minutes and depending on the total etching time again every hour to secure an even etching.

The effect of the etching as function of time is shown in Fig. 19, where the surface condition of the hole bottom is illustrated for etching times spanning from 0 to 16 h. The introduced flaws are gradually smoothen out and after 10 h the formation of crystals can be seen due to an inadequate cleaning, as some areas have not been etched properly. However, the change in surface condition is prominent.

5.2 Investigation on the strength by flexural testing

To study the effect of etching on the apparent strength of the hole, 8 different etching times were considered (5 h, 6 h, 7 h, 8 h, 12 h, 16 h, 20 h and 24 h) and compared to untreated holes. Each group consisted of 3 specimens tested in a ring-on-ring test, which is a common method for testing the flexural strength of brittle materials like glass. The test setup was built by two concentric rings, a load ring and a support ring, having diameters of 100 mm and 205 mm, respectively, mounted in an electromechanical universal testing machine. All experiments were performed at a loading rate of 12 kN/min with the hole placed centrally in the test setup on the tensile side.

Once the failure load is established, the equibiaxial flexural stresses within the load ring can be found from plate bending theory, see e.g. Timoshenko and Woinowsky-Krieger (1976)

$$\sigma_{\theta} = \sigma_r = \frac{3F_u}{2\pi h^2} \left[(1 - \nu) \frac{D_S^2 - D_L^2}{2D_e^2} + (1 + \nu) \ln \frac{D_S}{D_L} \right] \quad (5)$$

where F_u is the recorded peak load, h is the plate thickness, D_S is the support ring diameter, D_L is the load ring diameter and ν is the Poisson's ratio of soda–lime–silica glass ($\nu = 0.23$). Since all specimens tested had a rectangular geometry, an equivalent disc diameter, D_e , is defined according to ASTM C1499 (2015)

$$D_e = 0.54 (\ell_1 + \ell_2) \quad (6)$$

with ℓ_1 and ℓ_2 representing the side lengths of the specimen. It is recommended that the lengths should be within $0.98 \leq a/b \leq 1.02$ (squared geometry). However, this requirement was not met in this study and a FE-model was used to check the applicability of Eq. (6). The problem was modelled with four-noded shell elements (S4 in ABAQUS). A comparison between the analytical solution and the numerical model showed that results were achieved with a deviation below 2% using Eq. (6), even though the side length requirements were not met.

Equation Eq. (5) does not take into account the stress concentrations around the hole. From linear elastic theory it is well known that the stress concentration factor around a hole in a equibiaxial stress state is a factor of 2 as it follows from Eq. (1b). The failure stress, σ_f , at the hole surface can therefore be written as

Table 3 Flexural strength of the holes as function of etching time, tested in the ring-on-ring test setup

Specimen	Etching time (h)	F_u (kN)	σ_f (MPa)	σ_s^{top} (MPa)
1	0	13.39	125.72	−88.45
2		13.90	130.44	−91.41
3		13.86	130.06	−90.62
4		12.78	119.97	−90.62
5	5	14.96	140.46	−92.40
6		16.07	150.87	−90.62
7		16.28	152.84	−89.77
8	6	–	–	−94.01
9		33.63	315.68	−88.72
10		47.09	442.00	−91.21
11	7	46.29	434.55	−89.09
12		47.56	446.43	−87.20
13		37.44	351.47	−88.71
14	8	39.42	370.08	−88.63
15		37.37	350.82	−89.00
16		40.48	379.98	−89.55
17	12	47.70	447.76	−89.44
18		43.66	409.86	−88.41
19		40.33	378.59	−87.60
20	16	39.70	372.66	−89.54
21		45.81	430.03	−89.90
22		45.85	430.44	−90.70
23	20	40.22	377.51	−89.49
24		42.57	399.58	−89.68
25		44.47	417.48	−89.65
26	24	40.36	378.89	−90.03
27		42.85	402.28	−89.39
28		35.33	331.62	−89.85

One specimen with a hole etched for 6 h, needed to be rejected. The measured residual surface stress, σ_s^{top} is the mean of two orthogonal measurements

$$\sigma_f = 2\sigma_{\theta} \quad (7)$$

where σ_{θ} is the tangential stress within the load ring defined by Eq. (5).

The calculated apparent strengths of the hole boundaries for different etching times are presented in Table 3 together with the strengths of the untreated ones (etching time = 0 h) and the appertaining mean values are plotted together with the standard deviations in Fig. 20.

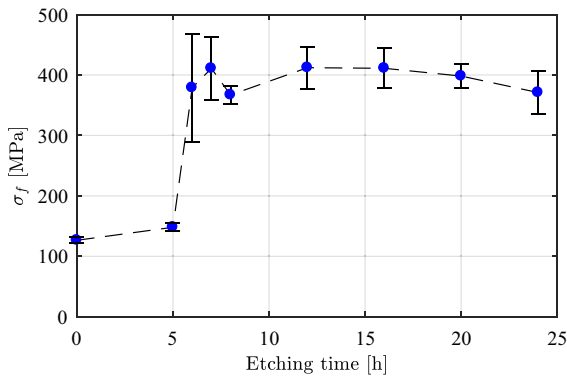


Fig. 20 Mean values of tested flexural strengths presented in Table 3 plotted together with the standard deviations

It follows from the results that the etching of the hole has a significant impact on the strength. After 5 h of etching, a small improvement is seen. An even better improvement is seen after 6 h where the flexural strength jumps from 148.1 to 378.8 MPa. However, etching the hole for more than 6 h leads to no further significant change in strength as it remains almost constant with about 400 MPa, resulting in an increase of 310% compared to the untreated holes.

An explanation of why a sudden change in strength is seen between 5 and 6 h could be that it takes time for the acid to reach the crack tip of a critical flaw produced by the drilling. In the beginning of the etching the acid only reacts with the glass around the hole boundary. With time it gets deeper and approaches the crack tip, but not enough to improve the strength significantly. Then the acid suddenly reaches the crack tip and smoothens it, resulting in a much higher strength as stress concentrations are minimised. This is thought to happen in the mentioned time span. Afterwards the degree of smoothness of the crack tip as function of etching time has no further influence on the strength.

Using etching for enhancing the strength of glass it is important to notice that scratching or even exposure to the surroundings may reduce the strength considerably. However, using it in the context of a joint in combination with an adhesive the etched parts should be sealed and protected. Further investigations on this matter should be considered.

6 Conclusion

The process of experimentally measuring the change in residual surface stress in tempered glass by drilling

has been given. It is shown that care should be taken when coating the strain gauge in order to protect it from the water used as cooling/cleaning agent when drilling. With the coating used here (a special silicone) the measurements and the drilling should not be carried out in the first 24 h after applying the coating. When the water is applied, a change in stress is also recorded, however, it becomes steady after less than a minute. Due to the steep variation in residual stress it is important to place the strain gauge as close to the hole as possible and to use strain gauges with a small measurement area and to remeasure the actual position.

The experimental results validate the finite element model used for investigating different geometric parameters. From the parametric study it can be concluded that drilling into the compressive zone of the tempered glass will not result in tensile stresses at the hole surface. However, the radial stresses will become zero due to the creation of a free surface (the hole boundary). For all geometric variations studied an increase in the apparent strength of the hole boundary is seen. Furthermore, even a small rounding of the bottom corner will lead to stress concentrations with finite stresses.

A successful etching technique has been developed to locally etch the holes as an attempt to strengthen them. From microscopic images it was shown that the flawed hole surfaces gradually could be smoothed when acid was applied for a certain time which has led to an improvement of the holes. Using a ring-on-ring test setup for testing the actual strength of the holes treated with different etching times has shown that after 6 h of etching the increase of strength had reached its maximum. It was possible to increase the strength with about 310% compared to the strength of untreated holes. However, more specimens are needed as the scattering of the results was somewhat large around the etching time where the sudden change in strength was seen.

The study demonstrates the effect of drilling into tempered glass. It shows a favourable redistribution of the residual stress state near the hole which makes it a feasible way of joining tempered glass without the need of holes drilled prior to the tempering process.

References

- Aben, H., Guillemet, C.: *Photoelasticity of Glass*. Springer, Berlin (1993)
- Anton, J., Aben, H.: A compact scattered light polariscope for residual stress measurement in glass plates. In: *Glass Processing Days*, pp. 86–88 (2003)
- ASTM C1499: Test Method for Monotonic Equibiaxial Flexural Strength of Advanced Ceramics at Ambient Temperature. Annual Book of ASTM Standards C1499-15, ASTM International, West Conshohocken, PA (2015)
- Kolli, M., Hamidouche, M., Bouaouadja, N., Fantozzi, G.: HF etching effect on sandblasted soda-lime glass properties. *J. Eur. Ceram. Soc.* **29**(13), 2697–2704 (2009). <https://doi.org/10.1016/j.jeurceramsoc.2009.03.020>
- Nielsen, J.H.: Drilling in tempered glass—modelling and experiments. In: *Engineered Transparency*, pp. 223–231 (2012)
- Nielsen, J.H.: Numerical investigation of a novel connection in tempered glass using holes drilled after tempering. In: *COST Action TU0905 Mid-term Conference on Structural Glass*, pp. 499–505 (2013). <https://doi.org/10.1201/b14563-68>
- Nielsen, J.H.: Remaining stress-state and strain-energy in tempered glass fragments. *Glass Struct. Eng.* **2**(1), 45–56 (2017). <https://doi.org/10.1007/s40940-016-0036-z>
- Nielsen, J.H., Bjarrum, M.: Deformations and strain energy in fragments of tempered glass: experimental and numerical investigation. *Glass Struct. Eng.* (2017). <https://doi.org/10.1007/s40940-017-0043-8>
- Nielsen, J.H., Olesen, J.F., Stang, H.: The fracture process of tempered soda–lime–silica glass. *Exp. Mech.* **49**(6), 855–870 (2009). <https://doi.org/10.1007/s11340-008-9200-y>
- Nielsen, J.H., Olesen, J.F., Poulsen, P.N., Stang, H.: Finite element implementation of a glass tempering model in three dimensions. *Comput. Struct.* **88**(17–18), 963–972 (2010a). <https://doi.org/10.1016/j.compstruc.2010.05.004>
- Nielsen, J.H., Olesen, J.F., Stang, H.: Characterization of the residual stress state in commercially fully toughened glass. *J. Mater. Civ. Eng.* **22**(2), 179–185 (2010b). [https://doi.org/10.1061/\(ASCE\)0899-1561\(2010\)22:2\(179\)](https://doi.org/10.1061/(ASCE)0899-1561(2010)22:2(179))
- Petzold, A., Marusch, H., Schramm, B.: *Der Baustoff Glas: Grundlagen, Eigenschaften, Erzeugnisse, Glasbauelemente, Anwendungen*, Hofmann, 3 edn (1990)
- Pourmoghaddam, N., Schneider, J.: Experimental investigation into the fragment size of tempered glass. *Glass Struct. Eng.* (2018). <https://doi.org/10.1007/s40940-018-0062-0>
- Proctor, B.A.: The effects of hydrofluoric acid etching on the strength of glasses. *Phys. Chem. Glass.* **3**(1), 7–27 (1962)
- Saha, C.K., Cooper, A.R.: Effect of etched depth on glass strength. *J. Am. Ceram. Soc.* **67**(8), C158–C160 (1984). <https://doi.org/10.1111/j.1151-2916.1984.tb19179.x>
- Timoshenko, S.P., Goodier, J.N.: *Theory of Elasticity*. Engineering Societies Monographs, 3 edn. McGraw-Hill, Auckland (1970)
- Timoshenko, S., Woinowsky-Krieger, S.: *Theory of Plates and Shells*. McGraw-Hill, New York (1976)
- Veer, F.A., Rodichev, Y.: The relation between pre-stress and failure stress in tempered glass. In: *Challenging Glass 4 and COST Action TU0905 Final Conference*, pp. 731–738 (2014)

Publisher's Note Springer Nature remains neutral with regard to jurisdictional claims in published maps and institutional affiliations.